

# Composition and Relative Volatility Estimation in Ethanol-Water Distillation Process through Quadratic Program Based Constrained Kalman Estimation Paradigm

*Sagi, Bharati*

*Department of Electronics and Instrumentation Engineering, VNR VJIET, Hyderabad, INDIA*

*Thyagarajan, Thangavelu\*<sup>+</sup>*

*Department of Instrumentation Engineering, MIT, Anna University, Chennai, INDIA*

**ABSTRACT:** Kalman filter is a classic iterative estimation technique widely used to estimate states and parameters of linear dynamic systems with white Gaussian measurement and process noises. However, if the measurement noises are predominant, resulting in poor signal to noise ratio, the estimator fails to provide allowable error covariance and optimal state estimation. In such circumstances, to enhance the estimation accuracy, measurement constraints need to be incorporated in the estimation routine. Through this work, a Quadratic Program based Constrained Kalman Estimation (QP-CKE) estimation sequence is proposed and developed to handle the additive measurement noise constraints. This is implemented by incorporating deconvoluted quadratic program with modified Kalman estimation paradigm to handle the constraint cost function. Composition estimation in a laboratory binary distillation process for ethanol-water mixture separation under steady state operating conditions is used as a case study. Noise augmented Two Input Two Output (TITO) linearized dynamic model of the process is established by inferring to Gaussian distributed tray temperature measurements and mixture vapor-liquid equilibrium data. The performance of this new estimator is tested for top and bottom composition estimation for step input excitation for reflux rate and reboiler power inputs under feed flow disturbances and the results are compared with that of conventional Kalman and Q adaptive Kalman estimators. Performance of the proposed estimator proves to be competent with reasonable computational speed and improved estimation accuracy. Also, relative volatility and vapor-liquid equilibrium trends are derived from estimated tray composition data and results are found in good relevance with that of the experimental data.

**KEYWORDS:** Distillation process; Gaussian noise; Quadratic Programmed Constrained Kalman Estimator (QP-CKE); Two Input Two Output (TITO) system; Adaptive Kalman Estimation (AKE).

---

\* To whom correspondence should be addressed.

+ E-mail: thyagu\_vel@yahoo.co.in

1021-9986/2023/1/310-320

11/\$/6.01

## INTRODUCTION

Model uncertainties are inevitable in data driven modelling due to inconsistent and noisy measurement plant data. Moreover, obtaining optimal state and output estimations under constrained environment is a tedious and time-consuming process. Due to this reason, the impact of physical constraints is ignored without further investigation in many estimator designs. Also, while using recursive filters like Kalman for state estimation, incorporating any kind of constraints on states would be a cumbersome task. Despite the computational burden, standard quadratic programming approach provides solutions to optimal state estimation under various linear- nonlinear equality and inequality constraints (Simon D. *et al.* (2003), 2005, Sarkar A. *et al.* (2014), Andersson L. *et al.* (2019)). In order to reduce the computational burden, modified density deconvolutional quadratic programming based standalone estimator is suggested by Yang R. *et al.* (2018) for Gaussian distributed errors under various constraints. For non-Gaussian distributed errors authors Prakash J. *et al.* (2008) have proposed a particle filter based recursive nonlinear constrained estimators. To further reduce the computational burden, Li R. *et al.* (2019) illustrated a twostep convex optimization solution for a non-convex inequality constrain problem.

There are various methods investigated in literature for imposing constraints on Kalman estimation paradigm. These are generally classified as estimate projection Kalman Filter (epKF), system projection Kalman Filter (spKF) and equality constrained Kalman Filter (ecKF). In epKF, the constrained estimation is achieved by projecting normally estimated states and error covariance on to the constraint subspace (Simon (2010)). In ecKF these projected state and error covariance are estimated in recursion (Teixeira, B *et al.* (2008) resulting in reduced error covariance at the cost of increased computational burden. On the contrary, spKF is achieved by projecting linear time invariant system on to the orthogonal null space such that it satisfies the given constrain. For improved accuracy and reduced the computational burden Chuanbo Wen *et al.* (2016) proposed a reduced order filtering approach.

Apart from using linear estimators like Kalman, Rouhani A., & Abur A. (2018), Farzi A. *et al.* (2009) illustrates dynamic state and parametric estimation using Unscented Kalman Filter (UKF) and Extended Kalman

Filter (EKF) under known constrain boundaries to address large measurement errors or outliers in states. Zhao J. (2019), illustrates UKF based constrained estimator to address equality and inequality constraints in a dynamic closed loop system.

Considering the benefits of estimation optimality with recursive filters like Kalman, in the present work we designed a modified deconvolution based QP approach for incorporating the constraints in proposed Kalman estimation routine. The performance of the resultant estimator is tested for dual compositions estimation using linearized empirical model of laboratory distillation process under Gaussian measurement noise.

## THEORETICAL SECTION

### Process description

This section provides the description of the distillation column, operational conditions, and sample chemical dynamics.

### Experimental setup

We have considered a stacked eight tray laboratory binary distillation column UOP3CC for this study. The schematic of that is represented in Fig. 1. We have operated the column under continuous mode in which case the feed mixture (ethanol and water) is fed continuously to the mid-section of the column through a peristaltic pump. The separation or distillation of the components in the mixture is achieved through maintaining unique boiling temperature across the column at which a vapor-liquid equilibrium is maintained between volatile (ethanol) and nonvolatile (water) components of the mixture. At this point more volatile component vaporizes and collected at the condenser. This condensed top product is recirculated through reflux valve back to the column until a pure component is released from the top. Reflux ration 'r' is one of the manipulative variables. The temperature in the column is maintained using an electric reboiler chamber placed at the bottom of the column which continuous boils up the liquid in the chamber. The vapor boil-up power 'q' is another manipulative variable used in this study. Both the manipulative variables 'r' and 'q' are continuously measured fed LabVIEW panel through PLC interface.

The column is equipped to measure temperatures at various junctions in the unit including the

temperatures across all the trays from T1 to T8 (top to bottom). It has an electrically operated reboiler with a power input 'q' required for the distillation with a power supply of 0-2.5KW. It has a reflux valve that can be operated with a reflux rate 'r' over the range 0-100%.

The column is operated at 101.32Kpa of pressure and with a continuous feed input of ethanol and water mixture (60%-40%) at tray 5. A peristaltic pump is operating at a speed of 200 RPM to pump the feed into the column. The vapors with enriched ethanol will reach the top of the column and collected as a distillate with an estimated composition of  $x_d$  mole fraction (0 to 1) at the top of the column and  $x_b$  mole fraction (0 to 1) at the bottom of the column.

The column is modeled with assumptions like constant molar flow across each tray, negligible liquid holdups, constant tray efficiencies of 0.6, and negligible heat loss through the walls of the column. Refer Table 1 for process specifications.

#### Mixture dynamics

Ethanol-water mixture is most commonly used non-ideal mixture having an azeotropic boiling temperature of about 78.2°C. Due to azeotropic phenomenon, the purity of the top product (ethanol) is limited to about 84% when operated at 101.32 kPa column pressure. Theoretical vapor-liquid equilibrium (VLE) and T-x-y diagrams for ethanol-water are used to establish a relationship between the effective tray temperatures and corresponding product compositions.

#### Sensor selection

The transient response dynamics of the column are captured through measuring tray temperatures T1 to T8 (top to bottom), reboiler temperature T9 and overhead vapor temperature T10 for a step change in two manipulative variables reflux rate and reboiler power inputs (r and q). The measurements come with sensor noises which are approximated to white Gaussian noise with seed value -1 and sampling rate 1.

The tray temperature profiles T1-T8, T9 and T10 are obtained from LabVIEW console connected to the UOP3CC, for various step input changes in reflux and reboiler power inputs. Reboiler power is gradually increased with a step size of 0.25 to 0.5 KW at complete

Table 1: UOP3CC Process specifications.

Specification	Details
Feed mixture	Ethanol (60%)-Water (40%)
Feed input	Continuous
Column Pressure (constant)	101.32 kPa/1 atm
Column diameter	50mm
Number of Trays/stacks	8
Feed inlet	At tray 5
Top to bottom tray temperature profile	T1 to T8 (0-150 °C)
Reboiler heat duty 'q'	0 -2.2 KW
% Reflux 'r'	0% – 100%
Speed of the feed pump	200 rpm (approx supplies 200 ml/min of feed)

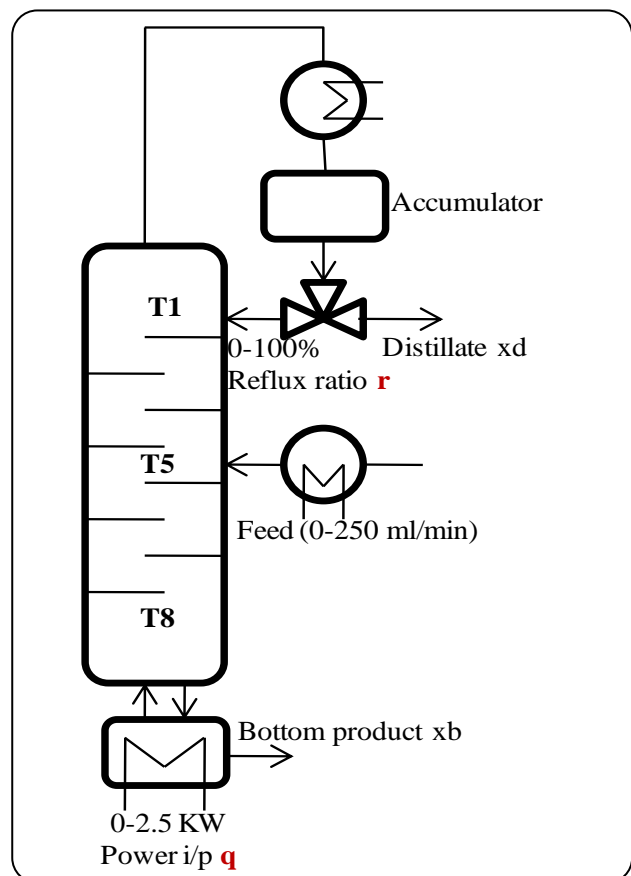


Fig. 1: Schematic of laboratory distillation column.

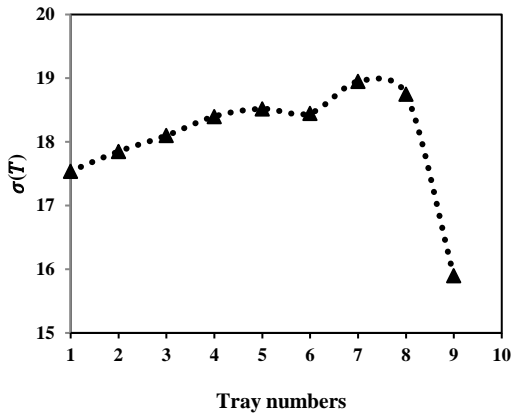


Fig. 2: Standard deviation of tray temperature measurements across the column (experimental).

reflux. The response in tray temperature profiles is measured from top tray temperature to bottom temperature and the reboiler temperature. Also, a standard deviation plot drawn from complete temperatures profile across the length column is plotted in Fig. 2. The temperatures T1(top tray) near the reflux and T8(bottom tray) near the reboiler indicate comparatively less standard deviation representing sensitive temperature trend towards the reflux and reboiler power inputs. The temperature T9 response is linearly increasing with reboiler input indicating the amount of heat gained by the sample. With this statistical analysis, the tray temperatures T1 and T8 can be considered as sensitive measurement locations for process modeling. These tray temperatures T1 and T8 will give a direct inference about the top and bottom compositions when enveloped with dynamics of direct composition measurement (offline). Further, Relative Gain Array (RGA) analysis is carried out for manipulative inputs *versus* selected tray temperatures T1 and T8 in the following session to understand the level of sensitivity shared across the two inputs and selected two outputs.

### Process modeling

The dynamic behavior of the column around the steady state operating point is sufficiently approximated using Linear Time Invariant (LTI) system in discrete time domain. The function n4sid in the system identification toolbox is opted for 2 state 2 output model building. First-order

butter worth filters with cut-off frequency 0.01rad/s.

The identified linear model is then coupled with first-order static linear first principal model to obtain the final linear model in terms of top and bottom compositions. The A, B and C matrices are obtained through system identification in MATLAB 2016a. Series of step changes in reflux ratio in the range of 60 to 95%, keeping the reboiler input constant *versus* T1 and T8 temperature profiles are considered as input and outputs around the steady state operating point (refer Table 1). The transfer functional model obtained for top and bottom compositions with respect to the model inputs reflux  $r$  and reboiler input  $q$  as given in (1). The transfer function models are then discretized into a state space model using the formulations (2) to (9). The LTI model thus developed can provide a fit value of 87% around the steady state operating point.

$$\begin{bmatrix} x_d \\ x_b \end{bmatrix} = \begin{bmatrix} P11 & P12 \\ P21 & P22 \end{bmatrix} \begin{bmatrix} r \\ q \end{bmatrix} \quad (1)$$

$$P11 = \frac{x_d}{r} = \frac{10.25}{16.75s + 1} = \frac{10.25}{16.7(z - 1) + 1} = \frac{10.25}{16.7z - 15.7} \Rightarrow x_{d_{k+1}} = \frac{15.7}{16.7}x_{d_k} + \frac{10.25}{16.7} = 0.94x_{d_k} + 0.613r_k \quad (2)$$

$$P12 = \frac{x_d}{q} = \frac{-18.9}{55s + 1} = \frac{-18.9}{155z - 54} \Rightarrow \dot{x}_d = 0.981x_{d_k} - 0.343q_k \quad (3)$$

$$P21 = \frac{x_b}{r} = \frac{8.2}{50s + 1} = \frac{8.2}{50z - 49} \Rightarrow x_{b_{k+1}} = 0.98x_{b_k} + 0.164r_k \quad (4)$$

$$P22 = \frac{x_b}{q} = \frac{-19.4}{10s + 1} = \frac{-19.4}{10z - 9} \Rightarrow x_{b_{k+1}} = 0.9x_{b_k} - 1.94q_k \quad (5)$$

By representing the above equations for state model, we get,

$$x_{d_{k+1}} = \begin{bmatrix} x1 \\ x2 \end{bmatrix}_{k+1} = \begin{bmatrix} 0.94 & 0 \\ 0 & 0.981 \end{bmatrix} \begin{bmatrix} x1 \\ x2 \end{bmatrix}_k + \quad (6)$$

$$\begin{bmatrix} 0.613 & 0 \\ 0 & -0.343 \end{bmatrix} \begin{bmatrix} r \\ q \end{bmatrix}_k$$

$$y1_k = [1 \quad -1] \begin{bmatrix} x1 \\ x2 \end{bmatrix}_k \quad (7)$$

$$\begin{bmatrix} x1 \\ x2 \end{bmatrix}_{k+1} = \begin{bmatrix} 0.98 & 0 \\ 0 & 0.9 \end{bmatrix} \begin{bmatrix} x1 \\ x2 \end{bmatrix}_k + \begin{bmatrix} 0.164 & 0 \\ 0 & -1.94 \end{bmatrix} \begin{bmatrix} r \\ q \end{bmatrix}_k \quad (8)$$

$$y2_k = [1 \quad -1] \begin{bmatrix} x1 \\ x2 \end{bmatrix}_k \quad (9)$$

Where:

k - Discrete time instances,

x1, x2, x3 and x4 - state variables

y1- distillate composition 'x<sub>d</sub>'

y2- Bottom composition 'x<sub>b</sub>'

u1 -%Reflux ratio 'r'

u2 - Reboiler power input 'q'

$$A1 = \begin{bmatrix} 0.94 & 0 \\ 0 & 0.981 \end{bmatrix}, B1 = \begin{bmatrix} 0.613 & 0 \\ 0 & -0.343 \end{bmatrix}, C1 = [1 \quad -1]$$

$$A2 = \begin{bmatrix} 0.98 & 0 \\ 0 & 0.9 \end{bmatrix}, B2 = \begin{bmatrix} 0.164 & 0 \\ 0 & -1.94 \end{bmatrix}, C2 = [1, -1]$$

### Estimator design

Consider a linear time invariant system and corresponding noise augmented system given by Equations (10) and (11).

$$x_{k+1} = Ax_k + Bu_k \quad (10)$$

$$y_k = Cx_k$$

$$x_{k+1} = Ax_k + Bu_k + w_k \quad (11)$$

$$y_k = Cx_k + v_k$$

Where k is the discrete time index,  $x \in R^{2 \times 1}$  is the state vector,  $u \in R^{2 \times 1}$  is a known input vector or a control input,  $y \in R^{1 \times 1}$  is a measurement vector and  $w \in R^{2 \times 1}$ ,  $v \in R^{2 \times 1}$  are process and measurement noise vectors. A- 2X2 state transition matrix, B-2X2 input matrix, C-1X2 observation matrix, and P- I<sub>2X2</sub> State error covariance matrix. 'Q' and 'R' are process and measurement noise covariance matrices.

### Kalman Estimation (KE)

A conventional kalman estimation routine with fixed error and measurement covariances is implemented *Bharati. Sagi, T.Thyagarajan (2021)*. The state and error estimation and optimization using regular Kalman filter is given as follows (12) to (14).

$$K_k = AP_k C^T (CP_k C^T + R_k)^{-1} \quad (12)$$

$$\hat{x}_{k+1} = A\hat{x}_k + Bu_k + K_k(y_k - C\hat{x}_k) \quad (13)$$

$$P_{k+1} = (AP_k - K_k CP_k)A^T + Q_k \quad (14)$$

The above eq.12 to eq.14) indicate that a prior knowledge of state and error covariances, R<sub>k</sub> and Q<sub>k</sub> is required in order to attain proper state estimation through regular Kalman filters. In practice these matrices are either assumed or unknown. This would cause severe inaccuracies while estimating critically noised systems or systems with uncertain measurements. In the following sections conventional adaptive and proposed QP-constrained Kalman estimation routines are presented to address these issues.

### Adaptive Kalman Estimation (AKE)

In most of the practical cases where measurement uncertainties and process noises exist, Kalman filter fail to generate estimate convergence since these uncertain system dynamics are not included in the filter model. To address these issues varieties of adaptive Kalman estimators are developed which will estimate and update state and error covariance matrices Q<sub>k</sub> and R<sub>k</sub> with changing system dynamics Dan Simon (2006), Gelb (1988), R.K. Mehra (1970), Mohamed, A and Schwarz, K (1999). To summarize, the adaptive filter variance and covariance matrices are updated for every new measurement enveloped with uncertain measurements and process noise. This is represented by the following set of equations (15) to (19). The error between received process measurements and predicted process measurements is evaluated to estimate and update Q<sub>k</sub> and R<sub>k</sub> matrices as follows.

$$e_{y_k} = y_k - \hat{y}_k \quad (15)$$

$$\hat{y}_k = G_k \hat{x}_k \quad (16)$$

$$\hat{G}_k = \frac{1}{N} \sum_{i=10}^k e_{y_i} e_{y_i}^T \quad (17)$$

$$\hat{R}_k = \hat{G}_k - M_k \hat{P}_k M_k^T \quad (18)$$

$$\hat{Q}_k = K_k \hat{G}_k K_k^T \quad (19)$$

Where

M<sub>k</sub> - Measurement design matrix

G<sub>k</sub> - Measurement innovation matrix

$\hat{P}_k$  and K<sub>k</sub> - are predicted covariance and state gain matrices respectively

e<sub>y<sub>k</sub></sub> - Measurement innovation at k<sup>th</sup> instance

N- Estimation window length

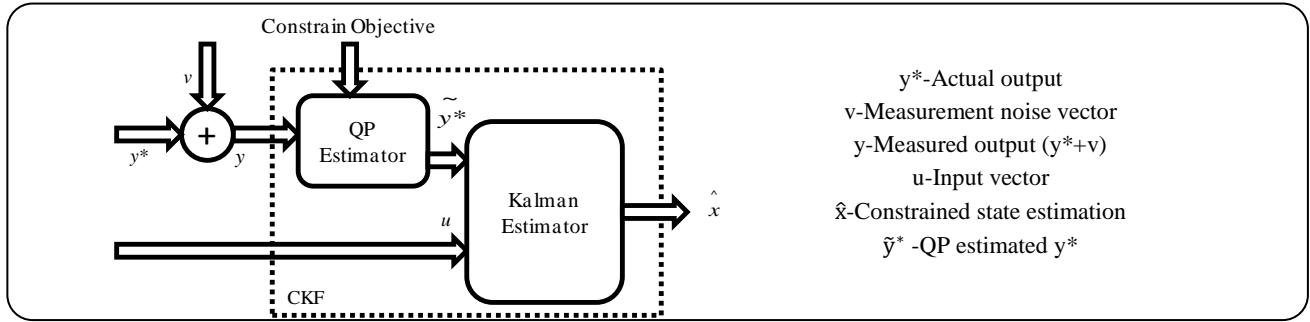


Fig. 3: Block diagrammatic representation of proposed QP-CKE.

### QP- Constrained Kalman Estimator (QP-CKE):

Kalman filter is known to provide optimal state estimation for linear dynamic systems with white Gaussian measurement and process noise. However, under model uncertainties and with state and observations constraints, it fails to provide optimal solutions. In this section we are proposing a reduced QP based constrained Kalman estimator to optimize the estimated constrained errors. Constraint problem is declared in such a way to obtain minimal error covariance by minimizing the density of errors accumulated across the zero mean.

With additive sensor noises, the measured process response can be expressed as  $y=y^*+v$ , where  $y^*$  is actual response of the process enveloped with additive white Gaussian noise  $v$  which is independent of  $y^*$ . In this section we used a modified density deconvolution based QP (Yang.R et al. (2019), Wolters M. A., & Braun W.J. (2017)) to propagate the Probability Density Function (PDF) of Gaussian errors over the declared equality constraints. We propose a cascaded constrained estimator model with regular Kalman filter (Fig. 3) to estimate the actual response of the process inferring to noisy observations of the plant. The Gaussian distributed error sequence generated after each prediction sequence in Kalman filtering routine has been deconvoluted using quadratic formulation. The PDFs of the observation vector when integrated to one, it provides non-negative solutions to the constraints in the QP formulation. The characteristic of density functions is that they are positive definite in nature and maintains optimal error even though the estimated constrained errors are not recursively used in the Kalman optimization routine.

For a random actual response vector  $y^*$  of the system, noisy observation vector  $y$  over  $n$  samples and observation error vector  $z$  with their respective PDFs are defined as  $f_{y^*}$ ,  $f_y$  and  $f_z$ . In order to obtain  $f_y$ , the following

deconvolution formulations are defined through Equations (15) to (19). The objective functions are described through Equations (20) and (21).

$$y^* = y_j^*; 0 \leq j \leq l \quad (20)$$

$$y_{\min}^* = \min(y_i; 1 \leq i \leq n) \quad (21)$$

$$y_{\max}^* = \max(y_i; 1 \leq i \leq n) \quad (22)$$

$$\delta = \frac{y_{\min}^* - y_{\max}^*}{1 - 1} \quad (23)$$

With an approximation

$$f_{y^*}(y^*) = f_{y^*}(y_j^*) \equiv f_{y^*,j} \text{ for } y^* \in \left[ y_j^* - \frac{\delta}{2}, y_j^* + \frac{\delta}{2} \right] \text{ and}$$

$$f_y(y) = \sum_{j=1}^l \int_{y_j^* - \frac{\delta}{2}}^{y_j^* + \frac{\delta}{2}} f_z(y - y^*) f_{y^*}(y^*) dy \quad (24)$$

The discrete constraint problem for the system represented in (5) and (6) is given below

$$f_y = D f_{y^*} \quad (25)$$

The state estimation error cost function is given by

$$\tilde{f}_y = \operatorname{argmin}_{f_y} \| \tilde{f}_{y^*} - f_y \|^2 + \lambda S(f_y) \quad (26)$$

The above constraint problem can be re written as state constraint cost function given by

$$\min_{\tilde{y}} (\tilde{y}^T \Sigma^{-1} \tilde{y} - 2 \hat{y}^T \Sigma^{-1} \tilde{y}) \quad (27)$$

For known noise distributions elements of the constraint matrix  $D$  can be evaluated using Eq. (28).

$$d_{ij} = \int_{(i-j-\frac{1}{2})\delta}^{(i-j+\frac{1}{2})\delta} f_z(y_i^* - y^*) dy^* \quad (28)$$

The term  $S(f_y)$  is a regularization term which penalizes ill conditioned  $f_y$  as well as reduces the oscillations due to the normalization term. Elements of matrix  $S(f_y)$  are evaluated

using Gaussian regularization method and regularization factor  $\lambda$  is a scalar quantity identified by observing the experimental data. For the collected set of experimental data,  $\lambda$  is evaluated using Yang R. *et al.* (2019) and best approximation is found at 0.00131.

#### Constrained Kalman filtering routine

Consider a linear dynamic system with white Gaussian measurement and process noises represented in Eq. (5) and 6. The following steps are executed in recursive estimation sequence incorporating measurement constraints through QP deconvolution. The initialization, state prediction and corrections sequences are as follows. Along with state and state noise covariance matrices, measurement noise covariance is also initialized in the Kalman routine. During update, estimated process real output vector  $\hat{y}$  is fed to the filter instead of noisy measurement vector  $y_m$ . The  $\hat{y}$  is estimated using QP formulation as discussed earlier. The optimized states are then recursively estimated by Kalman filter for any defined constrained objectives.

The proposed estimator works in two steps.

1. Estimating the actual process response from the available noisy measurements. This is achieved through QP density deconvolution method discussed through Equations (20) to (28).

2. State and output estimation is achieved through recursive Kalman filter using estimated responses coming from step1 approach.

The first step facilitates in primary noise minimization before feeding to the Kalman filter sequence. This will help in reducing the computational burden on recursive state optimization routine within Kalman filter. Since noise constraint and penalization terms are pre evaluated using approximated noise trend, Kalman estimation can converge within reasonable iterations. Measurement error density revisions in each Kalman iteration sequence is limited using an allowable error threshold.

Proposed QP-CKE algorithm is presented below through Equations (29) to (37).

#### Algorithm for proposed QP-CKE

Initialize

$$\hat{x}_{0|0} = E[x_0], P_{0|0} = var[x_0] \text{ and} \quad (29)$$

$$P_k = \int_{-\alpha}^{+\alpha} E[\tilde{f}_y^* - f_y], Q_k, R_k, S_k \text{ and } \lambda_k$$

Predict

$$\bar{\hat{x}}_k = A\bar{\hat{x}}_{k+1} + B \quad (30)$$

$$\bar{P}_k = A P_{k+1} A^T + Q_k \quad (31)$$

Correction

$$K_k = \bar{P}_k C^T (C \bar{P}_k C^T + R_k)^{-1} \quad (32)$$

$$\hat{x}_k = \bar{\hat{x}}_k + K_k (y_k - C \bar{\hat{x}}_k) \quad (33)$$

$$P_k = (I - K_k C) \bar{P}_k \quad (34)$$

Updating

$Q_k$  and  $R_k$  as defined in equations 15 to 19

Where error for optimization is

$$e_{y_k} = \tilde{y}_k^* - \hat{y}_k^* \quad (35)$$

$$\tilde{y}_k^* = G_K \hat{x}_k \quad (36)$$

$\tilde{y}_k^*$  - denoised process response botained through QP stage

$\hat{y}_k^*$  - Kalman estimated response

$$\hat{f}_y = \operatorname{argmin}_{f_y^*} \| \tilde{f}_{y^*} - f_y \|^2 + \lambda S(f_y) \quad (37)$$

Such that

$$\sum \delta 1^T f_y = 1 \quad \forall f_y \geq 0$$

## RESULTS AND DISCUSION

In this study, a linearized dynamic plant models (refer Equations (1) to (4)) are empirically derived from continuously operated distillation plant (UOP3CC) data. Noisy tray temperature observations over 2500 uniformly distributed samples are considered for this study and same are scaled down to 250 samples for presentation convenience. These sensor measurement noises are approximated to Gaussian white noise with zero mean and standard deviation 1. Operational parameter range for taking the steady state performance analysis of various estimators is given in Table 2.

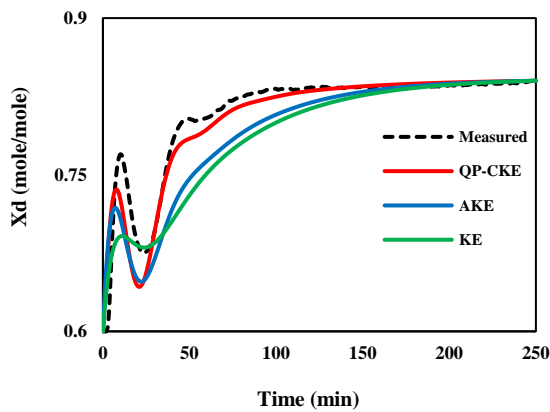
Results showcased in Fig.4.a to 4.d indicate the estimated distillate and bottom compositions developed from denoised plant model. Improved and smoother performance is noticed with proposed Kalman estimation sequence when compared to its counterparts.

Fig.5. a, b and c, project the estimated composition profiles when the system is under simultaneous excitation by dynamic reflux rate, reboiler power input and feed flow disturbances. Because of the smaller bottom composition profile (around 0.3 to 0.6 mole fraction), sensor noises predominantly override the actual signal. It is evident from

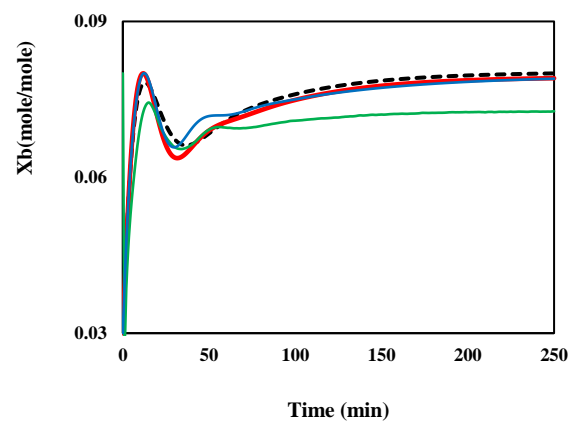
**Table 2: Operating range for process parameters.**

Parameter	Steady state operable Range
Reflux Rate % r	50% to 95% opening
Reboiler Power input %q	1.5 KW to 2.2 KW
Feed Flow %f	150 – 200 ml/min
Distillate Composition (steady state)	0.7 to 0.84 mole fractions
Bottom Composition (steady state)	0.03 to 0.08 mole fractions
Steady state temperature Range	72 °C to 100 °C

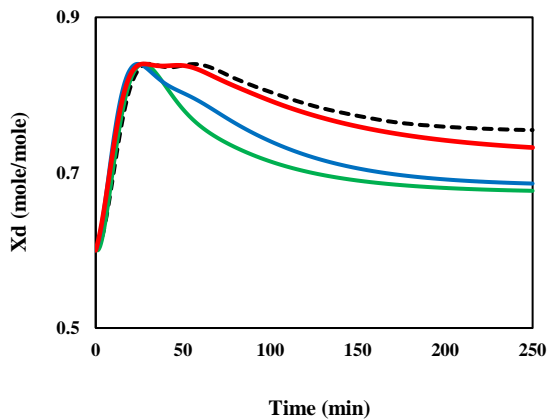
a). Measured and estimated distillate composition ( $X_d$ ) profiles for 5% step increment in reflux rate, %r



b). Measured and estimated bottom composition ( $x_b$ ) profiles for 5% step increment in reflux rate, %r



c). Measured and estimated distillate composition ( $x_d$ ) profiles for 5% step increment in vapor boil up, %q



d). Measured and estimated bottom composition ( $x_b$ ) profiles for 5% step increment in vapor boil up, %q

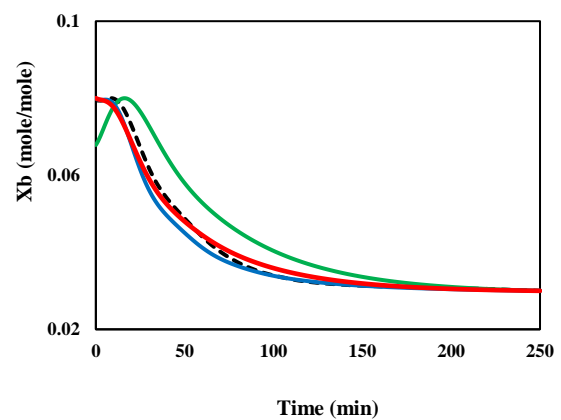


**Fig. 4: Measured and estimated composition profiles under 5% step increment in reflux rate 'r' and vapor boil up 'q' (without noise).**

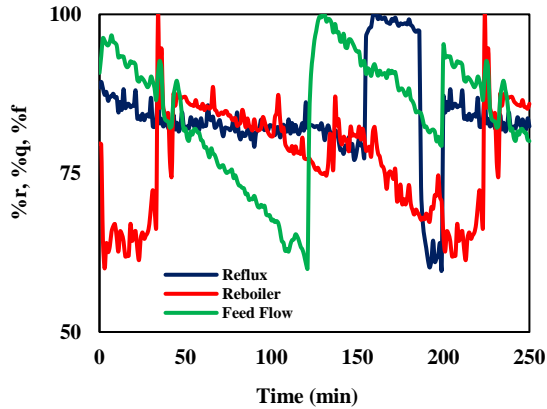
these graphs that a smoother accurate estimation is achievable through proposed QP-CKE even under combined noisy excitation for the process, which is a more realistic case.

Composition profile across eight distillation trays

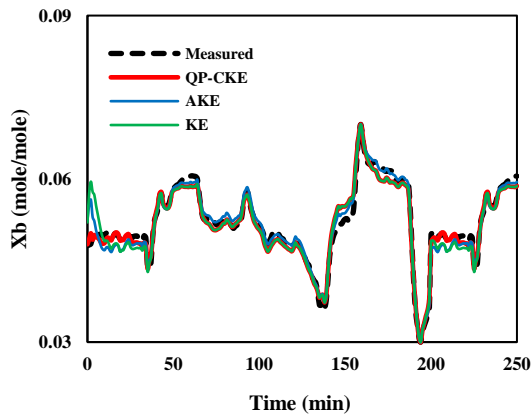
is also derived and presented in Fig. 7. Proposed Kalman estimation provided smooth estimation compared to conventional Kalman and adaptive Kalman techniques even for smaller signal to noise ratio. A useful information about relative volatility ethanol-water ( $\alpha$ ) is derived from



a). Combined noisy excitation profiles (% reflux  $r$ , %reboiler power  $q$ , %feed flow  $f$ )



b). Distillate composition profile under process and measurement noises



c). Bottom composition profile under process and measurement noises

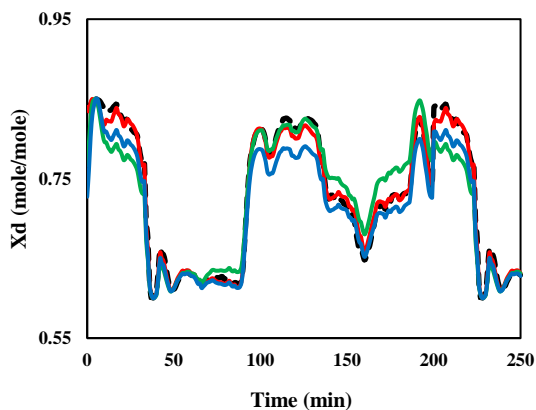


Fig. 5: Measured and estimated composition profiles under noisy excitation.

the tray composition profile and the estimation accuracies are compared and analyzed (refer. Fig. 8). The computational time and convergence rate are reasonably maintained well within the limits for QP-CKE when compared to that of KE and AKE. The reduced QP formulation penalized the accuracy and computational time for given set of samples. The proposed estimator performance is quantitatively evaluated using Root Mean Square Error (RMSE) metric for both noise and de noised process and measurement conditions. And results are tabulated in Table 3. It is evident from this table that QP-CKE reasonably improves the estimator performance even under noisy measurements.

The performance of the QP-CKE over unconstrained KE and AKE is quantitatively projected using Table 3. The values shown are average root mean square error values over 10 simulations. It is evident from the graphical presentations (Figs. 4,5,7 and 8) and below indicated quantitative performance comparisons (refer Table 3) that QP-CKE shows an improved performance over the regular Kalman and adaptive Kalman routines without imposing much computational burden. But the performance of these filters is highly model dependent and are vulnerable to model uncertainties. Also, the constraints considered are minor deviations in the sensor measurements, but do not address the large sensor biases and failures.

## CONCLUSIONS

An analytical method for incorporating constraints in Kalman estimation routine using deconvolutional QP is proposed and results are demonstrated. The known constraints like minimizing measurement noises in the present case study can be incorporated in Kalman routine without increasing filter's computational burden. However, proper choice of regularization parameter will greatly influence the accuracy of estimation. Also, the accuracy and smooth performance can be obtained using a smaller number of samples. The recurring Kalman estimation routine further optimizes the estimation. Use of PDF incorporated non-negative approximation of errors and hence provides the flexibility to incorporate inequality constraints as well. Dual composition estimation profiles indicate that in either of the cases, the QP-CKE have shown smoother responses compared to KE and AKE methods. It is observed that the QP-CKE can track smaller variations

Table 3: Performance comparisons of estimators KE, AKE and QP-CKE.

Parameter Estimated	Estimation error (RMSE)					
	Without noise			With noise		
	KE	AKE	QP-CKE	KE	AKE	QP-CKE
Distillate composition $x_d$	0.225	0.154	0.045	0.378	0.227	0.094
Bottom Composition $x_b$	0.316	0.236	0.108	0.567	0.311	0.194
Average relative volatility Ethanol-Water: $\alpha_{ave}$	0.279	0.185	0.081	0.456	0.233	0.105

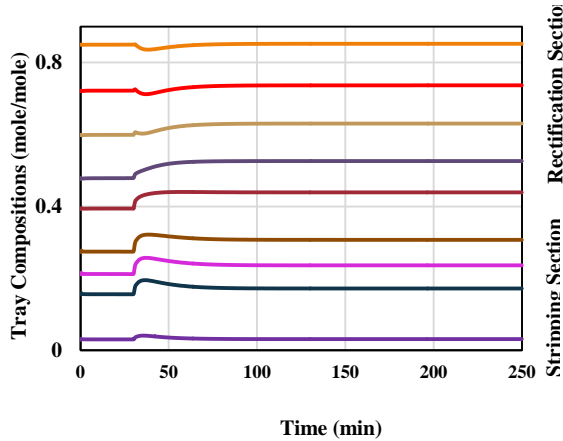


Fig. 1: Estimated composition profile across all trays (bottom to top).

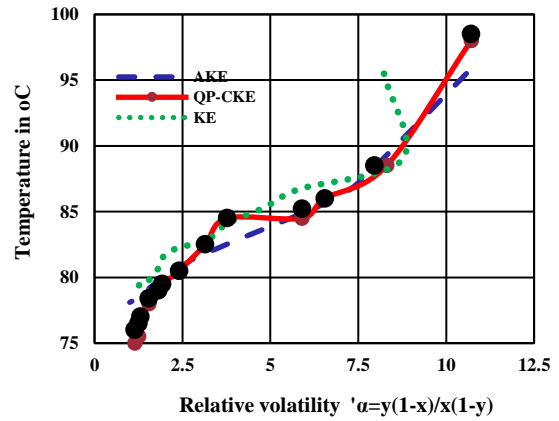


Fig. 8: Ethanol Relative volatility profile derived from experimental and estimated data.

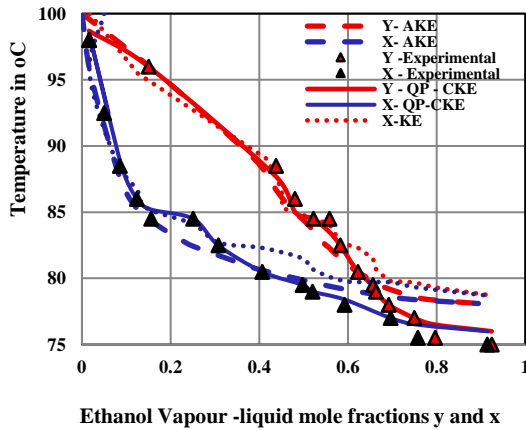


Fig. 2: Vapor-liquid equilibrium profile derived from experimental and estimated data.

in the state dynamics and are visible through bottom composition estimation plot.

Further investigation is required to realize the applicability of the proposed method over nonlinear subspace. Also, our future works are oriented towards

extending and testing the present estimator performance for online estimation to incorporate direct data driven control.

### Nomenclature

$y^*$	Actual output vector of the process over n samples
$y$	Noisy measurement/observation vector over n samples ()
$v$	Measurement/observation noise vector
$f_y(.)$	Probability density function vector in 'y'
$f_{y^0}$	Initial value of $f_y$
$f_y(.) = (f_y * f_z)(y)$	Probability density function vector in 'y'
$f_z(.)$	Probability density function vector in 'z'
$D$	$n \times n$ convolution matrix with elements $d_{ij}$
$\sim$	Unconstrained estimation representation
$\wedge$	Constrained estimation representation
$\lambda$	Regularization factor (calculated from data)
$S$	Error density covariance matrix
$\delta$	Discretization parameter over the length of samples l

Received Dec. 28, 2021 ; Accepted : Apr. 4, 2022

## REFERENCES

- [1] Simon D., Chia T., [Kalman Filtering with State Equality Constraints](#), *IEEE Trans. Aerosp. Electron. Syst.*, **39**: 128–136 (2003).
- [2] Simon D., Simon D.L., [Aircraft Turbofan Engine Health Estimation Using Constrained Kalman Filtering](#), *Journal of Engineering for Gas Turbines and Power*, **127**(2): 323 (2005).
- [3] Sarkar A., Mallick B.K., Staudenmayer J., Pati D., Carroll R.J., [Bayesian Semiparametric Density Deconvolution in the Presence of Conditionally Heteroscedastic Measurement Errors](#), *Journal of Computational and Graphical Statistics*, **23**: 1101–1125 (2014).
- [4] Prakash J., Patwardhan S.C., Shah S.L., [Constrained State Estimation Using Particle Filters](#), *IFAC Proceedings Volumes*, **41**(2): 6472–6477 (2008).
- [5] Li R., Magbool Jan,N., Huang B., Prasad V., [Constrained Multimodal Ensemble Kalman Filter Based on Kullback–Leibler \(KL\) Divergence](#), *Journal of Process Control*, **79**: 16–28 (2019).
- [6] Simon D., Simon D.L., [Constrained Kalman Filtering via Density Function Truncation for Turbofan Engine Health Estimation](#), *International Journal of Systems Science*, **41**(2): 159–171 (2010).
- [7] Mehra R.K., “[On the Identification of Variances and Adoptive Kalman Filtering](#)”, *IEEE Trans. Automatic Control*, **AC-15**(2): 175- 184 (1970).
- [8] Mohamed A., Schwarz K., [Adaptive Kalman Filtering for INS/GPS](#), *Journal of Geodesy*, **73**: 193–203 (1999).
- [9] Teixeira B., Chandrasekar J., Palanhandalam-Madapusi H.J., Torres L., Aguirre L.A., Bernstein D.S., [Gain-Constrained Kalman Filtering for Linear and Nonlinear Systems](#), *IEEE Transactions on Signal Processing*, **56**(9): 4113–4123 (2008).
- [10] Wen C., Cai Y., Liu Y., Wen C., [A Reduced-Order Approach to Filtering for Systems with Linear Equality Constraints](#), *Neurocomputing*, **193**: 219–226 (2016).
- [11] Rouhani A., Abur A., [Constrained Iterated Unscented Kalman Filter for Dynamic State and Parameter Estimation](#), *IEEE Transactions on Power Systems*, **33**(3): 2404–2414 (2018).
- [12] Mohammadnia V., Salahshoor K., [A New Comprehensive Sensor Network Design Methodology for Complex Nonlinear Process Plants](#), *Iranian Journal of Chemistry and Chemical Engineering (IJCCE)*, **31**(3): 145-156 (2012). doi: 10.30492/ijcce.2012.5961
- [13] Zhao J., Mili L., Gomez-Exposito A., [Constrained Robust Unscented Kalman Filter for Generalized Dynamic State Estimation](#), *IEEE Transactions on Power Systems*, 1–1 (2019).
- [14] Sagi B., Thangavelu T., “[Data Driven Modelling for Dual Composition Estimation in Binary Distillation Process](#)”, *4th International Conference on Computer, Communication and Signal Processing (ICCCSP)*, 1-6 (2020). doi: 10.1109/ICCCSP49186.2020.9315278.
- [15] Yang R., Apley D.W., Staum J., Ruppert D., [Density Deconvolution with Additive Measurement Errors using Quadratic Programming](#), *Journal of Computational and Graphical Statistics*, 1–20 (2019).
- [16] Wolters M.A., Braun W.J., [Enforcing Shape Constraints on a Probability Density Estimate Using an Additive Adjustment Curve](#), *Communications in Statistics - Simulation and Computation*, **47**(3): 672–691 (2017).